 FDMP, vol.12, no.2, pp.86-101, 2016

Wall-Pressure Fluctuations of Modified Turbulent Boundary Layer with Riblets

Hayder A. Abdulbari [1,2], Hassan D. Mahammed[1], Z. Hassan and Wafaa K. Mahmood[3]

Abstract An experimental investigation was carried out to study the response of a turbulent pressure drop fluctuations to longitudinal groove riblets, involved two configurations being triangular and spaced triangular grooves with height 600, 800, 1000 μm and peak to peak spacing 1000 μm and 2000 μm respectively. Experiments were therefore performed at free stream velocity up to 0.44 m/sec, which were corresponding to Reynolds number (Re) 53000. The development of the obtained turbulent layer downstream of the grooves was then compared with the results from the corresponding smooth-wall case. To conclude, the effect of the spaced triangular riblets on the turbulent characteristics seemed to be more pronounced than the effects of the triangular riblets.

Keywords: Drag reduction, skin friction, riblets, geometry.

1 Introduction

The modification of fluid flows by riblets, especially in the vicinity of and inside their grooves, is more commonly treated in the literature, where the aim is to reveal the underlying drag reduction mechanism and to better understand turbulence.

The reduction of skin friction by modifying the structure of a turbulent boundary layer near the wall was the original idea behind the introduction of riblets. To this end, extensive research has been conducted to study the influence of riblets on turbulence structures and mean flows qualitatively and quantitatively as well as experimentally and numerically.

The influence of riblets on turbulence structures and mean flows has been investigated by Hooshmand, Youngs, Wallace, and Balint (1983), Choi (1989), Baron and Quadrio (1993), Park and Wallace (1994), Wang, Lan, and Chen (2000), Alfonsi (2008), Yulia, Pierre, and Yves (2008), Kim (2011), Lian and Meelan (2012, 2014).

It is agreed that there is a slow flow with low skin friction in the valleys of the grooves of drag-reducing riblets. The riblets' grooves appear to dampen the lateral motion and spreading of low-speed streaks. The turbulence intensity and the Reynolds stress are decreased. With drag-reducing riblets, there is an upward shift in the log-law velocity

[1] Faculty of Chemical and Natural Resources Engineering, Universiti Malaysia Pahang, Gambang 26300, Kuantan, Pahang, Malaysia,

[2] Center of Excellence for Advanced Research in Fluid Flow, Universiti Malaysia Pahang, Gambang 26300, Kuantan, Pahang, Malaysia

[3] Department of Manufacturing and Metallurgy, University of Technology, Baghdad, Iraq

profile due to an increase in the thickness of the visous sublayer and a displaced virtual origin. However, with drag-increasing riblets, there is a downward shift in the log-law velocity profile. Few changes in the skewness and flatness factors of the velocity fluctuations have been observed. The effects of rib surfaces on the turbulent flow in rectangular channels and circular tubes have been extensively studied in literature (Abdulbari, et al. 2013, 2015, 2016; Dean & Bhushan, 2010; Fish & Lauder, 2006; Gad-el-Hak, 1996).

Choi (1988) studied the wall pressure fluctuations in a wind tunnel to modified turbulent boundary layer with riblets. The tunnel had a test section of (4.8 $m \times 2.4\ m \times 15\ m$) and 0.5 % flow speed controlled by a feedback control system. The results of this study were drawn comparing with a smooth surface. The results revealed that surface modifications are reduced RMS intensity up to 4 %. The reduction appeared as a result of a decrease in turbulence intensity within a small volume near a riblet surface.

Reidy and Anderson (1988), conducted experimental studies in 3M riblets in a high-speed water tunnel over a flat plate in turbulent flow. Moreover, the second experiment has been in 6-inch diameter pipeline system. 3M vinyl riblets have been used in both systems with height (h) and spacing (s) of V-groove $h=s= 76.2\ \mu m$. The results show a maximum drag reduction 8.1 %. Wilkinson and Lazos (1988) studied the direct drag and hot wire measurements on thin element riblet arrays. This experiment was conducted in a low-speed air using hot wire data. The studied revealed that thin element riblet causes counter-rotating vortex pairs containing 130 viscous wavelengths. With variation in riblet spacing, turbulence intensity magnitude and location of peaks also shifted. The study used rectangular riblets with 0.05*mm* two dimensions and two separate tunnels to measure direct drag and hot wire data. A 2x6 inch tunnel with test section dimensions of $51 \times 152 \times 457$ *mm* was used to measure hot wire data. Direct drag was measured in another tunnel with $178 \times 279 \times 914$ *mm* test section. In both tunnels, the floor was used as the test surface. The drag data measurement also shown the vortex activity caused by non-dimensional wide range of riblet spacing

Frohnapfel, Jovanović, and Delgado (2007) studied the near wall turbulence in functional space and provided remarkable results of drag reduction of 25 % over the ribbed surface using velocity fluctuation method for measurements. Lee & Choi (Lee & Choi, 2008)a study using PIV measuring technique produced similar results of Wilson and Lasoz that indicated the causation of vortex rotating formation by v-groove surface and drag reduction was also observed. Shark skin inspired riblet structures were studied by Büttner and Schulz (2011), using high temperature resistant nickel alloys. This study was conducted for application of drag reduction using riblets in aero engines. The study used different sizes of riblets that were dependent on temperature, pressure and velocity of flowing medium. The reduction of sheer wall stress was studied in oil channel which proved that fabricated riblet structures can be used to produce effective drag reduction.

An investigation was conducted by Dean and Bhushan (2012) on the effect of riblets in internal rectangular duct flow. Blade riblets with groove height *(h)* of 254 μm with three ratios of height to space equal to 0.3, 0.5, and 0.7 were fabricated. Their results showed increasing in pressure drop for all tasted rib surfaces comparing to smooth surface and no drag reduction recorded. Dean& Bhushan concluded that the reason of rib surface did not

show an overall benefit in reducing the drag, due to riblets dimensions as presented in their paper not beneficial in duct flow of that nature and dimensional characteristic.

Bixler and Bhushan (2013b) later on published his results on the difference in surface roughness and their effect on the pressure drop. The core of Bixler &Bhushan work was to study blade and sawtooth riblets' effects with continuous and segmented configurations in air and water closed channel. The results show an improvement in reducing the pressure drop in both air and water turbulent versus laminar flow. It was found the maximum pressure drop reduction of 34 % in water flow and 26 % in air flow.

An experiment conducted by Prince, Maynes, and Crockett (2014) combined the drag reduction techniques of superhydrophobicity and groove riblets. The pressure drop was measured in a turbulent flow in canals with ribbed walls and with superhydrophobic walls, and the results were combined. The groove riblets showed a maximum drag reduction of 3 % for a Reynolds number of 1.1×10^4 Moreover, 3.2 % when combined with superhydrophobic walls. In contrast, a maximum drag reduction of 7 % was found when the surfaces were combined. The riblets were ostensibly 18 μm wide, 80 μm height, 160 μm apart, and arranged parallel to the flow. Drag-reducing surfaces were fabricated with silicon wafers that were inserted into a channel comprising a control segment containing smooth wafers and a test section containing ornate wafers. Several challenges were met during the investigations of drag reduction over ribbed surfaces in wind and water channels. In wind channels, because the viscous sublayer was less than 0.1 mm thick, the turbulent shear stress was slight and difficult to measure accurately based on force balance.

Investigations have revealed the features of surface textures in which the efficacious in many different applications, such as enhancing flow in pipes and reduce the drag surfaces, self-cleaning types of surface, dicing, commercial aeroplane, fighter plane, underwater vehicles and others applications (James, Paul, & Richard, 2000; Klocke, Feldhaus, & Mader, 2007; Liu & Jiang, 2012; Moalem-Maron, Semiat, & Sideman, 1980; Naterer, Glockner, Thiele, Chomokovski, Venn, & Richardson, 2005; Nishimoto & Bhushan, 2012; Wang, Song, & Pan, 2005; Xu & Carey, 1990). With such wide-ranging of applications, bring a magnificent attention from worldwide to this field.

Nonetheless, several challenges face surface textures and disabling this technology to be translated into industrial applications. Where there are no certain design (shape and dimensions) of riblets that can be used for all type of applications, due to turbulent regime where the turbulence coherent structure are completely random, as the viscous sublayer and the streamwise vortices are different from fluid to another due to properties of the fluid and the application circumstances. Moreover, the difficulties in riblets' manufacturing for a laboratory scale and for large-scale applications, where for the last one, it is much more difficult due to the long cross section that has to be covered with a groove (Dean, 2011). Furthermore, the accuracy of riblets' manufacturing for experimentation has been a field of study in its right as there are plenty of techniques that may use to fabricate micro-grooves (Chen, Hsieh, Chou, Lin, Shen, & Tsai, 2007; Worgull, 2009). Moreover, some other challenges such as material type and the fabrication process as rolling, grinding, etching and laser etching (Bixler & Bhushan, 2013a).

In the present work, an experimental investigation is conducted to examine the effect of changing the valley height of grooves on the drag reduction performance of Triangular and

spaced triangular groove shapes. Moreover, investigation on the effect of changing peak-to-peak groove spacing from 1000 µm in triangular groove shapes to 2000 µm in spaced triangular groove shapes. The present work was performed in a flow channel system with flow capability and where a Reynolds number of 53000 can be reached. This setup provides the needed intensive-turbulent flow environment to test the drag reduction performance of the investigated riblets.

2 Experimental set-up and measuring techniques

2.1 Experimental apparatus and riblets fabrication

Establishment of the influence of longitudinal triangular riblets on the improvement of the pressure characteristics of the chosen models is the primary purpose of the current work. The effectiveness of the drag reduction of the selected riblet dimensions is tested in the current work through a closed loop system. This is illustrated in Fig. 1. One tank rectangular in shape with a length of 500 *mm* width of 300 *mm* depth of 520 *mm* and capacity of 70 *litters*, is contained in the system. A pump that is capable of driving the main fluid at a rate of 36 m^3/hr, PVC pipes with 2 inches in size, flow meter, pressure transducers and the square channel is also contained. There was the usage of tap water, which continuously changed after every test. The centrifugal pump is used to pump water from the supply tank. After that, it is taken to the PVC pipes and then to the transparent channel and then back to the supply tank.

The designing and fabrication of the square channel of the experiment rig have been done, where there has been the inclusion of four transparent polycarbonate plates that has dimensions (2×0.12×0.01) *m* that has been applied for channel fabrication. Fabrication of every section of the channel was done through acrylic welding. The pressure drop was measured through the channel after four pressure tabs were located at its bottom surface. To attain a complete turbulence flow, 0.16 *m* test sections of the said tabs were located after two sections of 0.55 *m.* Six ball valves, which were well situated at the points of entry and exit of the water were contained in the system. Their purpose was to control water flow. There was connection of the pressure transmitters to the initial test section that had a length of 0.16 *m.* Then, the pressure drop for the section on the smooth plate and rib surface was recorded. To remove every vibration in the experimental equipment, care was observed when fluctuating pressure measurement in the channel wall was being taken. The riblet surfaces have been manufactured through Aluminum sheets with dimensions (9.53×90×3000) *mm*. This has been achieved by cutting the plate into the size of the test section (8×80×160) *mm* with CNC machine. After prepared the plates, WEDM machine was used to fabricate the triangular groove. A Brass Wire with a diameter of 250 μm was used as an electrode to erode a workpiece.

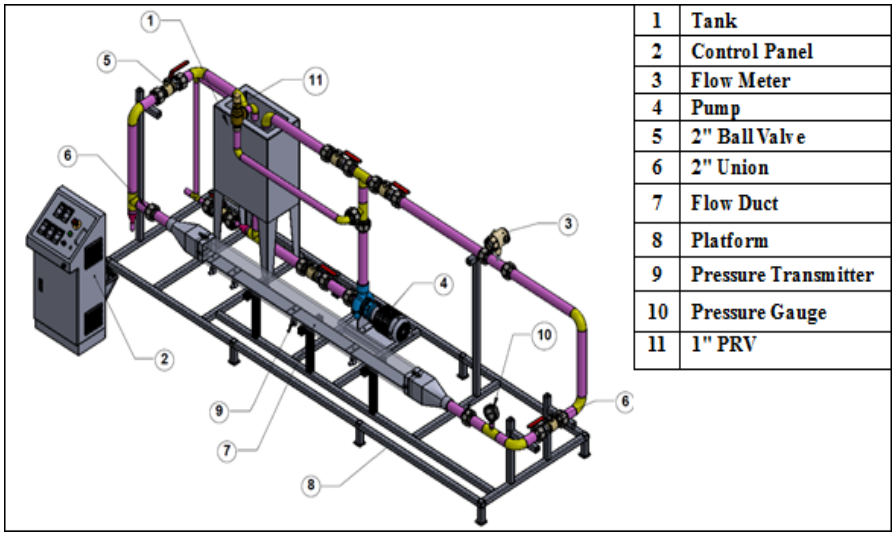

Figure 1: Shows the experimental rig

Two sets of riblet surface were fabricated which allowed inspection and measurement of drag reduction effects of riblets spanning as well as a range of flow velocities and turbulence conditions. A sample of fabricated riblet surface is shown in Fig. 2 that illustrates grooves that are defined by peak height (h), peak-to-peak spacing (s). The first set of riblets (three riblets) which was fabricated included shaping triangular riblets which have equal peak-to-peak spaced of 1000 µm but varied valley heights 600 µm, 800 µm, and 1000 µm. The second set (three riblets) were triangular riblets built upon the first set by manipulating the overall scale of the riblets with incrementally increasing the spacing of the riblets to 2000 µm. In this way, the s^+ range of the riblets which is known to be beneficial in external flows was studied throughout the range of flow rates achievable by the channel. This size-adjustment allowed the study of riblets from Reynolds numbers of 13000 to 53000 based on channel hydraulic diameter and ensured that the majority of the turbulent range of the system was studied within the operational range of the riblets.

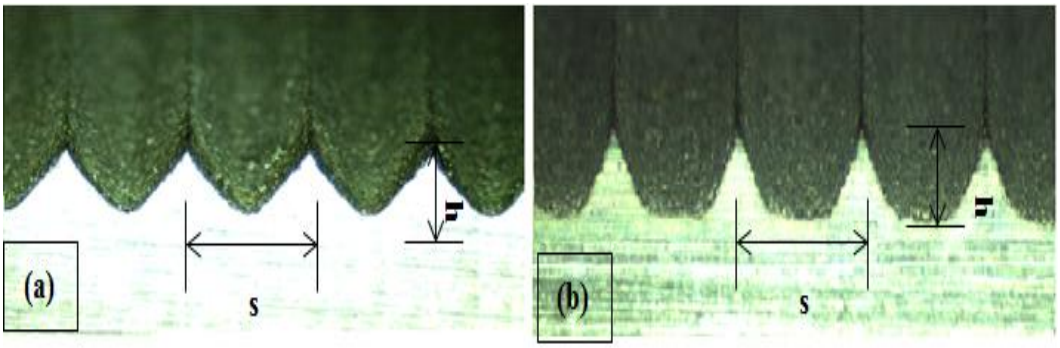

Figure 2: Fabricated triangular riblets where (a) triangular (b) spaced triangular

2.2 Measurements

The skin friction coefficients (Cf) and Reynolds numbers (Re) calculated from wall shear stress and flow rate measurements by using following equations,

$$Cf = \frac{2\tau_w}{\rho\, u^2} \text{ and } Re = \frac{u\, D_h}{\upsilon} \quad (1)$$

Where (u) is mean velocity $(m/\sec)$, (υ) is the kinematic viscosity of water $(m^2/\sec)$, (ρ) is the density of water (Kg/m^3) and (τ_w) is the wall shear stress in a fully developed pipe flow was defined by Perry et al. (Green, 2008). This equation relates the wall shear stress to the pressure drop during the turbulent flow inside pipelines.

$$\tau_w = \frac{\Delta p\, D_h}{4L} \quad (2)$$

The height and spacing of the grooves in wall units are calculated by using Walsh (1982) identification in terms of wall units as non-dimensional height (h^+) and spacing (s^+), as;

$$h^+ = \frac{h\, u}{\nu}\sqrt{\frac{C_f}{2}} \text{ and } s^+ = \frac{s\, u}{\nu}\sqrt{\frac{C_f}{2}} \quad (3)$$

where (C_f) is local skin friction coefficient, (s) is peak to peak spacing of riblets and (h) is the valley to peak height of riblets.

The percentage drag reduction (DR %) is defined as:

$$\text{DR\%} = \left(\frac{\Delta P_{Smooth} - \Delta P_{riblet}}{\Delta P_{Smooth}}\right) \times 100 \quad (4)$$

The diameter used in the calculations Reynolds number and friction coefficient is defined as Hydraulic diameter $D_h = 4\frac{A}{p}$ Where (A) is area section of the duct and (p) is wetted perimeter of the duct.

3 Experiment results and discussion

As per the theory, the effect of longitudinally grooved surfaces on wall-pressure fluctuations can be estimated by calculating the effect first on a smooth flat plate and then on a ribbed plate. To get a well-defined result, the Reynolds number and surface roughness of both the plates should be the same.

The first thing that needs to be addressed before the measurement is the time series of pressure. We can analyze the time domain by plotting a graph of the sequence of data points of the signal obtained. This will give an accurate description of the time scale, rate, and complexity of the flow. The pressure signal, on the other hand, depends on the random fluctuations which are roughly near the mean pressure value.

The turbulent flow relies on fluctuations in three factors, namely, pressure, acceleration and shear stress. All three are directly associated with position and time. These fluctuations directly affect the velocity and pressure terms in the momentum and energy equations which will show varied differences. Fig. 3, show the pressure drop fluctuations over the smooth and riblet plates at Reynolds number 5.3×10^4.

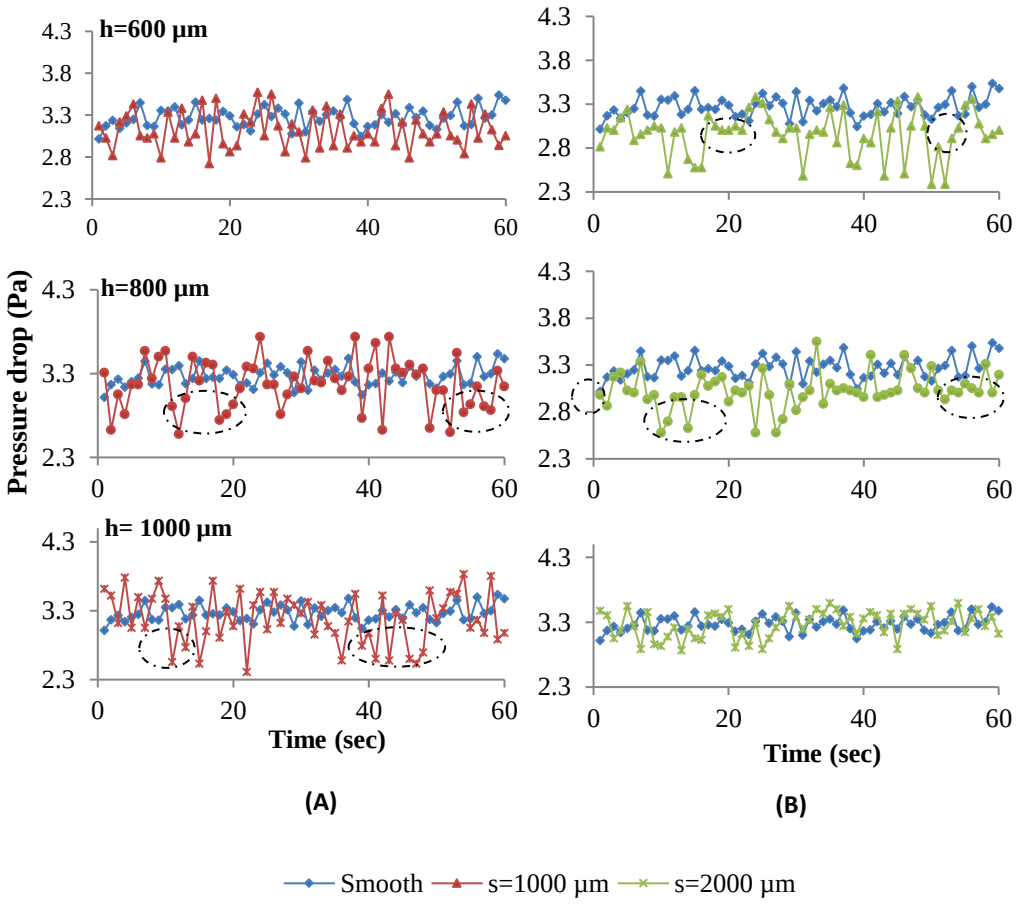

Figure 3: Pressure fluctuation time series at Reynolds number 5.3×10^4 for smooth and riblet surfaces where (A) Triangular riblets and (B) spaced triangular riblets.

The current experiment requires investigation of a certain mechanism that manages the drag reduction and behavior of the grooved surfaces. Thus, there is a measurement of the pressure drop readings of every type of surface and the flow rate, where this is performed at similar 60s. Consequently, two differing groups of fluctuations that play part in the wall pressure as peer the recommendation offered by the whole body of results occur (Beresh, Henfling, Spillers, & Pruett, 2013; Gao, Liu, Yang, & Tan, 2010; Johnsson, Zijerveld, Schouten, van den Bleek, & Lackner, 2000).

Two groups of fluctuations that make up the wall pressure, the first one is made up of large-scale disturbances that are of low-frequency. Such disturbances come from the surrounding portions of the boundary layer and goes up to within the unsteady potential flow. The large-scale disturbances remain consistently on course with the character of the interface of the potential flow which is outside the boundary layer.

The second group of pressure fluctuation, on the other hand, is made up of small-scale disturbances that are of high-frequency and are considered to have a relation with the burst-

sweep cycle of events. Such disturbances are also noted to follow the wall pressure fluctuations of large-amplitude.

The large-amplitude wall pressure peaks, according to the results of the conditional sampling techniques on signals of pressure and velocity that are simultaneously acquired, are realized to have relation to the shear layer structures found in the buffer region, and have an association with the bursting process in flat-plate turbulent boundary layers, turbulent flows of pipes, as well as direct numerical simulation turbulent channel, flows (Snarski & Lueptow, 1995).

According to Karangelen, Wilczynski, and Casarella (1993), there's consistency between the frequency of the busting events in the buffer regions and that of occurrence of large-amplitude wall pressure events taking place in a flat-plate boundary layer.

An investigation was carried out by Thomas and Bull (1983) about a possible relationship between the large-scale structure in the outer portions of the flow and the pressure peaks of the near-wall high amplitude. The two correlated the portions of the signals as well as sampling the low-frequency portion of the high-frequency pressure peaks after separating the pressure signals into low frequency as well as high-frequency portions. Their conclusion was that there was interdependency between the both frequencies disturbances (the high and the low), and this was not caused at all by the large-scale structures in a much as they are linked to the bursting process.

Another investigation on the bursts and the large-scale motion relationship was carried out by Kobashi and Ichijo (1986); Snarski and Lueptow (1995). Their conclusion, unlike that of Thomas and Bull (1983), stated that it is the interaction of the large-scale motion of the wall that results in bursts.

A survey by Kline and Robinson (1990) concluded that there is a weak interaction between the inner and outer layers to an extent the events in the inner layer are “phase-locked to and triggered by the motions of the outer region.”

The pressure drop performed on the surface showed readings that are stable while having a turbulence frequency lower than other surfaces. It was seen that the pressure drop point is below the smooth surface pressure drop but with irregular readings. Now the structured surfaces exhibit pressure readings which are higher in amplitude and smooth surface readings which are lower in amplitude. It is seen that the structured surfaces have a lower pressure drop on average but in some points, it may be higher.

This is because the low pressure drop arises when the pressure drops stabilize for a certain time and then returns to the smooth surface readings. The same pattern repeats several times which explains the low-pressure drops on average. The profiles of the pressure fluctuation time series under different conditions were illustrated as in Fig. 4. The turbulent characteristics in the square channel were fully embodied. Generally, the fluctuation pressure profile with different Reynolds numbers at smooth and riblets, the fluctuation of pressure time series obviously increased as the Reynolds number of the inlet flow increased over riblets compared to smooth surface. But the amplitudes average values of riblet is less than amplitudes average values of smooth surface.

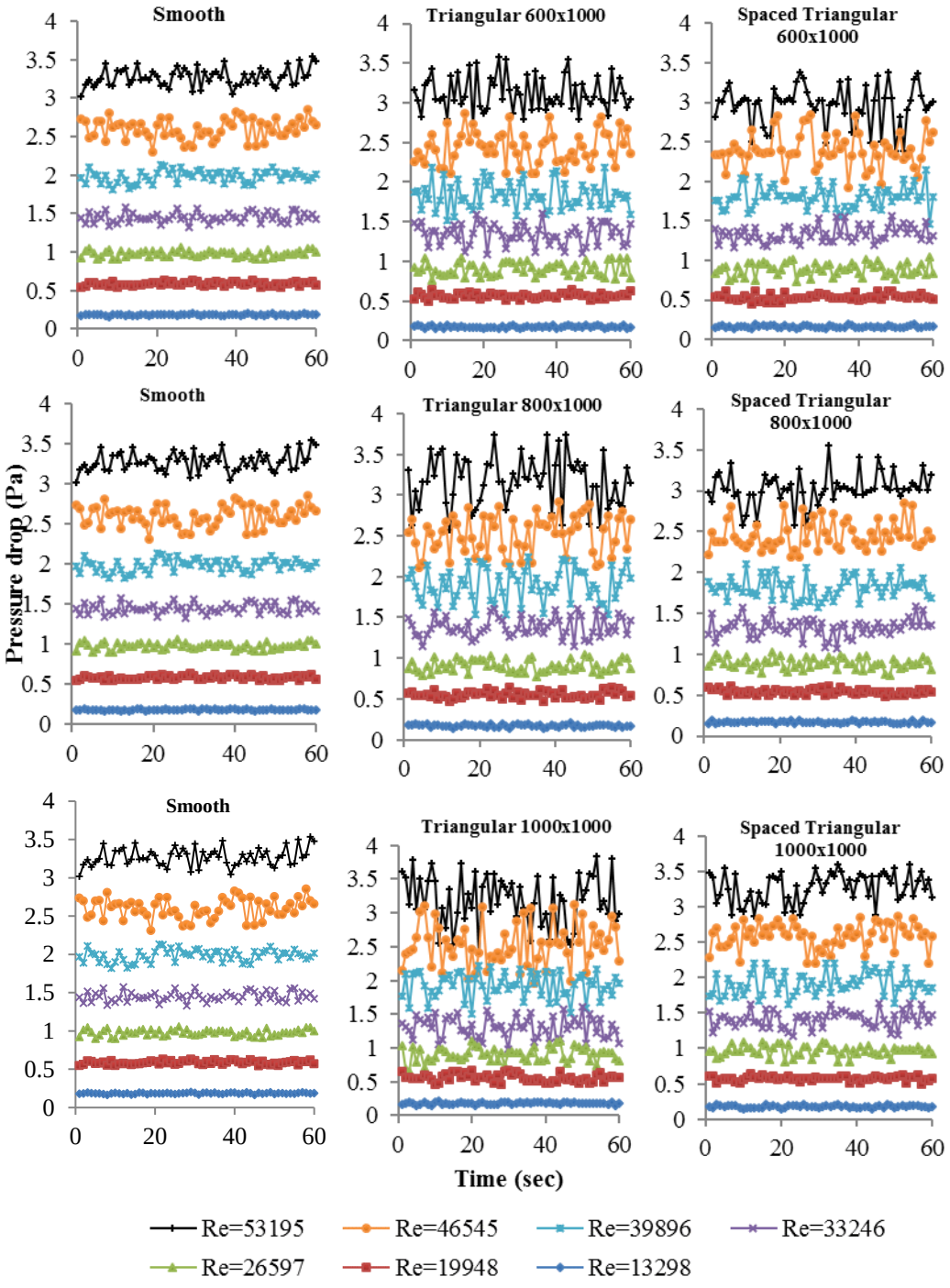

Figure 4: The profiles of pressure fluctuation time series under different Reynolds number for smooth and riblets with selected dimensions

These experiments deal with the Reynolds numbers between 13000 and 5000. Fig. 5, discuss the pressure drop measured across the smooth plate and all triangular riblet surfaces. This figure shows that increasing the Reynolds number with the different riblet geometries increases the rate of the pressure drop for the tested plates.

Two well-defined zones spotted out. First, the convergence zone in which the pressure drop of the grooved and smooth surfaces are similar, i.e., when the Reynolds number is in the range from 1.3×10^4 to 1.9×10^4, shows a steady increase in the rate of pressure drop with increasing Reynolds number. Second, the pressure drops of the tested plates continue to increase and start to diverge when the Reynolds number ranges from 2.3×10^4 to 5.3×10^4. In contrast, most of the results for riblets with different longitudinal dimensions demonstrate a beneficial trend compared with the smooth surface for the entire range of Reynolds numbers tested. In general, it must be noted of that the trends of riblet type's dimensions with height 600, 800 and 1000 μm are below the pressure drop of the smooth plate which show a capability to reduce the drag force. The peak height of 600 μm of both type's of riblets shows extraordinary low values of pressure drop compared to other tested surfaces. Moreover, Peak height of 800 μm comes the second in lowering the pressure drop compared to other tested surfaces. However, with 1000 μm shows no sensible impact of pressure drop compares to a smooth surface.

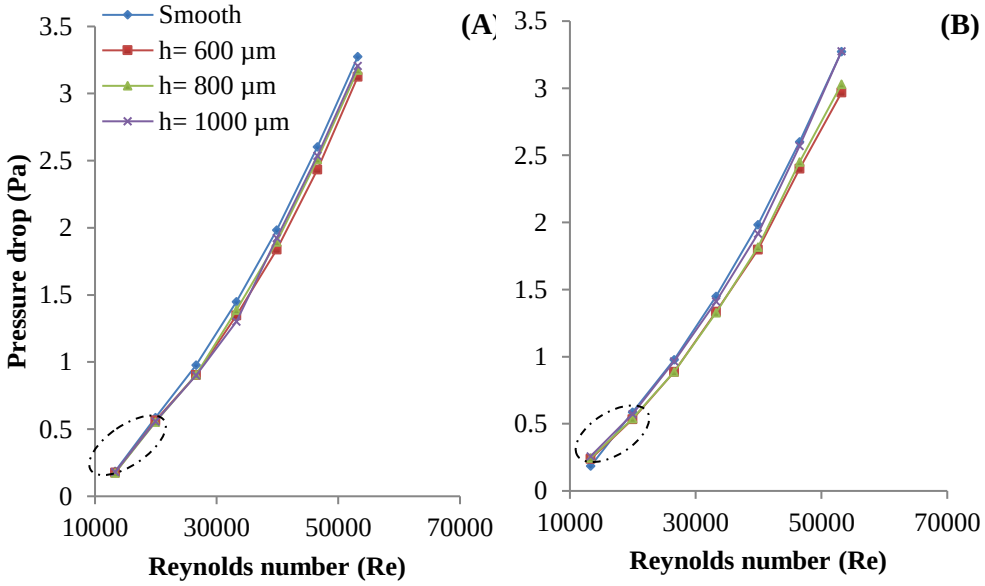

Figure 5: Pressure drop comparison over smooth and riblets surfaces where (A) Triangular riblets and (B) spaced triangular riblets.

Fig. 6, demonstrate the effect of non-dimensional space (s^+) and Reynolds number on the percentage of drag reduction with different triangular and spaced triangular riblet heights. the data obtained for Reynolds number range of Reb≈13000–53000. The riblet spaces in nondimensional wall units were then estimated from Eq. 3. and the percentage of drag reduction was estimated from Eq. 4.

The present measurements of riblet drag reduction show that the percentage drag reduction increases by increasing the $s^+$and Reynolds number for most of the tested riblets until a certain value where the percentage drag reduction start to descend. Which means increasing the turbulence spectrum and reaching a maximum point or maximum performance "which might be considered as optimum performance for this point only". After that and by a further increase in the value of the s^+ and Reynolds number start to decline in most cases due to the strong action of these turbulent structures over riblets, where riblets no longer could modify these structures, which is dependent on the properties of the particular boundary layer. However, the best performance for riblets was in range of s^+ equal to 15-20 wall unit and for Reynolds number range equal to 30000 to 40000.

Typically, increasing the groove height from 600 to 1000 µm did not increase the percentage of drag reduction. The results show a distinguishable difference when comparing the effect of the groove height to the same groove type and spacing. Fig. 6. (A), show the best performance of triangular groove with height 600 µm then triangular groove with height 800 µm as second best performance. However, for height 1000 µm even show a high percentage of drag reduction, but yet the curve line was not stable enough to consider it best performance.

Fig. 6. (B) show the performance of triangular space riblets where groove height of 600 µm was the best then 800 µm which follows same behavior of triangular riblets even there is different in peck to peck spacing.

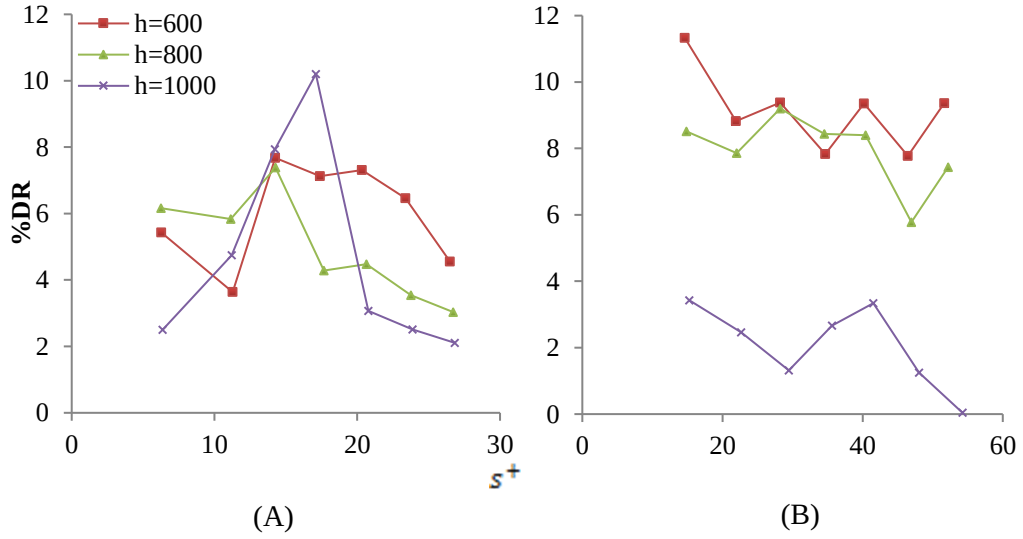

Figure 6: Drag reduction obtained in square channel where (A) Triangular riblets and (B) spaced triangular riblets.

The results of the experiment work are used to identify possible drag reduction mechanisms for riblets in turbulent flow. Different mechanisms have been identified in the literature, and each mechanism is based on numerical or experimental results.

The drag reduction mechanism is the most complicated part of this phenomenon and continues to be the subject of much argument and criticism. A few issues cause difficulty

in providing a clear idea on a certain mechanism that may control the drag reduction in channel flow: (i) the unstable and sometimes "strange" behavior of the fluid in turbulent flow, (ii) the highly chaotic movement of fluid molecular masses in different directions, and (iii) the absence of a clear and exact mapping of the turbulence inside the channel.

One of the suggested mechanisms is the role of groove riblets as impeded of coherent vortex structure. Where riblets are considered as significant devices that reduce drag in turbulent flow. As the boundary layer vortices are blocked by riblets to hinder them from settling in between the tips of the riblet in the valleys (Choi, 1993).

Usually, riblets have diameter vortices, which is about 30 dimensionless value that concern riblet tips' spacing and thus, they are regarded as effective devices (Benhalilou & Kasagi, 1999). This advantage also discusses the significance of a decrease drag envelope that is 5 < h^+, s^+ < 30. However, drag reduction can be reversed or increased when there is an increase in the wetted area, which occurs when there is smaller spacing in contrast to the lower bound. On the other hand, the vortices will settle in the valleys when there is larger in contrast to the upper bound. The blocking behavior of vortex should be visible since the sharp riblet dimensions will currently be in the decreasing phase of the drag.

Another suggested a mechanism, is that riblets push away the coherent structures near the wall. When the riblets are approached by boundary layer vortices, the riblet peak starts shedding the vorticity conflicting sign Thus; this is caused by the spanwise cross flow produced by the vortices as well as the separation at the tips of the riblet, and therefore, vortices are generated. This means there is the induction of an upward flow component at the riblet tip. By Goldstein, Handler, and Sirovich (1995), the coherent structures of turbulent flow are pushed away from the wall of the riblet by the upward speed component that is above the tips of riblet.

Furthermore, Choi, Moin, and Kim (1993), Goldstein et al. (1995), and Bechert, Bruse, Hage, Van Der Hoeven, and Hoppe (1997) indicates that there is an alternative concept of illustrating decrease drag behavior. It thus indicates that the volume of momentum mixing in the riblet valleys is reduced by the damping of the cross-flow that exists between the riblets. The results show that there is little dynamical activity in the valley and in particular below the riblet midpoint as it identified as a dead area.

Thus, the influence of the riblets can be coupled with geometrical properties as they decrease the drag in turbulent flow. The spanwise cross-flow damp, even if there is vertical cross-flow damp, marks to be the primary focus in this case. A reduction can be seen in the strength of the vortices that are shed near the top, where this is determined by the strength of the riblet tip shape and cross-flow, can be identified when there is a higher damping of the component through strongly aimed riblet geometry.

A strong momentum combination is identified in the riblet valleys in the secondary vortices. However, there is washing out of fluid energy from the valleys as well as pumping of the high momentum fluid into the valleys. In other words, more drag reduction can be observed when the secondary vortices are killed or their strength reduced.

Nevertheless, push away effect is seen to contradict with this concept. There would be a decrease in the upward velocity component that is above the riblet tip if the vortices are

reduced. This then would lead to a reduction in the push away the effect of the riblets and as a result, mechanism positive effect on the performance would be reduced.

4 Conclusions

The present study investigates the behavior of flows and the drag reduction of ribbed surfaces using pressure drop measurements. The experimental results clearly indicate that the most stable and consistent pressure drops that have clear drag-reducing effects (low-pressure drops) occur for grooves height of 600 μm. Moreover, the performance in term of shape was space triangular with a peak to peak space 2000 wherein the highest percentage of drag reduction was 9%.

Acknowledgments This work was supported financially by University Malaysia Pahang (UMP) through the Fundamental Research Grant.

References

Abdulbari, H. A., Mahammed, H. D., & Hassan, Z. B. Y. (2015): Bio-Inspired Passive Drag Reduction Techniques: A Review. *ChemBioEng Reviews*, 2(3), 185-203.

Abdulbari, H. A., Yunus, R. M., Abdurahman, N. H., & Charles, A. (2013): Going against the flow—A review of non-additive means of drag reduction. *Journal of Industrial and Engineering Chemistry*, 19(1), 27-36.

Abdulbari, H. A., Rosli M Yunus, A Charles. (2016): A Turbulence-Altering Pseudo-Surface for Enhancing the Flow in Pipes. *Chem. Eng. Comm.*, 203(2), 278-286.

Alfonsi, G. (2008): PASSIVE TECHNIQUES FOR CONTROL OF TURBULENCE IN WALL-BOUNDED FLOWS. 15(3), 217-234.

Baron, A., & Quadrio, M. (1993): Some preliminary results on the influence of riblets on the structure of a turbulent boundary layer. *Int. J. Heat Fluid Flow*, 14(3), 223-230.

Bechert, D. W., Bruse, M., Hage, W., Van Der Hoeven, J. G. T., & Hoppe, G. (1997): Experiments on drag-reducing surfaces and their optimization with an adjustable geometry. *J. Fluid Mech.*, 338, 59-87.

Benhalilou, M., & Kasagi, N. (1999): Numerical prediction of heat and momentum transfer over micro-grooved surface with a nonlinear k–ε model. *Int. J. Heat Mass Transfer*, 42(14), 2525-2541.

Beresh, S. J., Henfling, J. F., Spillers, R. W., & Pruett, B. O. M. (2013): Very-large-scale coherent structures in the wall pressure field beneath a supersonic turbulent boundary layer. *Physics of Fluids*, 25(9), 095104.

Bixler, G. D., & Bhushan, B. (2013a): Fluid Drag Reduction with Shark-Skin Riblet Inspired Microstructured Surfaces. *Adv. Funct. Mater.*, 23(36), 4507-4528.

Bixler, G. D., & Bhushan, B. (2013b): Shark skin inspired low-drag microstructured surfaces in closed channel flow. *J. Colloid Interface Sci.,* 393, 384-396.

Büttner, C. C., & Schulz, U. (2011): Shark skin inspired riblet structures as aerodynamically optimized high temperature coatings for blades of aeroengines. *Smart Mater. Struct.,* 20(9), 094016.

Chen, S.-W., Hsieh, J.-C., Chou, C.-T., Lin, H.-H., Shen, S.-C., & Tsai, M.-J. (2007): Experimental investigation and visualization on capillary and boiling limits of micro-grooves made by different processes. *Sensors and Actuators A: Physical,* 139(1-2), 78-87.

Choi, H. (1993): *Turbulent drag reduction: Studies of feedback control and flow over riblets.* (Ph.D), Stanford University & Thermosciences Division TF-55., Ann Arbor United States. Available Database Provider Name of Database database.| (Document Number)

Choi, H., Moin, P., & Kim, J. (1993): Direct numerical simulation of turbulent flow over riblets. *J. Fluid Mech.,* 255, 503-539.

Choi, K. S. (1988): The Wall-pressure Fluctuations of Modified Turbulent Boundary Layer with Riblets. In H. W. Liepmann & R. Narasimha (Eds.), *Turbulence Management and Relaminarisation* (pp. 149-160): Springer Berlin Heidelberg.

Choi, K. S. (1989): Near-wall structure of a turbulent boundary layer with riblets. *J. Fluid Mech.,* 208(-1), 417.

Dean, B., & Bhushan, B. (2010): Shark-skin surfaces for fluid-drag reduction in turbulent flow: a review. *Philosophical Transactions of the Royal Society of London A: Mathematical, Physical and Engineering Sciences,* 368(1929), 4775-4806.

Dean, B., & Bhushan, B. (2012): The effect of riblets in rectangular duct flow. *Appl. Surf. Sci.,* 258(8), 3936-3947.

Dean, B. D. (2011): *The Effect of Shark Skin Inspired Riblet Geometries on Drag in Rectangular Duct Flow.* (MSc), The Ohio State University, Ohio. Available Database Provider Name of Database database.| (Document Number)

Fish, F. E., & Lauder, G. V. (2006): Passive and Active Flow Control by Swimming Fishes and Mammals. *Annual Review of Fluid Mechanics,* 38(1), 193-224.

Frohnapfel, B., Jovanović, J., & Delgado, A. (2007): Experimental investigations of turbulent drag reduction by surface-embedded grooves. *J. Fluid Mech.,* 590, 107-116.

Gad-el-Hak, M. (1996): Modern Developments In Flow Control. *Applied Mechanics Reviews,* 49(7), 365-380.

Gao, P.-z., Liu, T.-h., Yang, T., & Tan, S.-c. (2010): Pressure drop fluctuations in periodically fluctuating pipe flow. *J. Marine. Sci. Appl.,* 9(3), 317-322.

Goldstein, D., Handler, R., & Sirovich, L. (1995): Direct numerical simulation of turbulent flow over a modeled riblet covered surface. *J. Fluid Mech.,* 302, 333-376.

Green, D. W. (2008): Perry's chemical engineers' handbook (Vol. 796): McGraw-hill New York.

Hooshmand, D., Youngs, R., Wallace, J. M., & Balint, J. L. (1983): An experimental study of changes in the structure of a turbulent boundary layer due to surface geometry changes. *Paper presented at the 21st Aerospace Sciences Meeting*,Reno, Nevada

James, L., Paul, K., & Richard, R. (2000): Low Reynolds number loss reduction on turbine blades with dimples and V-grooves *38th Aerospace Sciences Meeting and Exhibit*. USA: American Institute of Aeronautics and Astronautics.

Johnsson, F., Zijerveld, R. C., Schouten, J. C., van den Bleek, C. M., & Leckner, B. (2000): Characterization of fluidization regimes by time-series analysis of pressure fluctuations. *Int. J. Multiphase Flow,* 26(4), 663-715.

Karangelen, C. C., Wilczynski, V., & Casarella, M. J. (1993): Large Amplitude Wall Pressure Events Beneath a Turbulent Boundary Layer. *J. Fluids Eng.*, 115(4), 653-659.

Kim, J. (2011): Physics and control of wall turbulence for drag reduction. *Philosophical Transactions of the Royal Society of London A: Mathematical, Physical and Engineering Sciences,* 369(1940), 1396-1411.

Kline, S., & Robinson, S. (1990): Quasi-coherent structures in the turbulent boundary layer. I-Status report on a community-wide summary of the data. *Near-Wall Turbulence,* 1, 200-217.

Klocke, F., Feldhaus, B., & Mader, S. (2007): Development of an incremental rolling process for the production of defined riblet surface structures. *Production Engineering,* 1(3), 233-237.

Kobashi, Y., & Ichijo, M. (1986): Wall pressure and its relation to turbulent structure of a boundary layer. *Exp. Fluids,* 4(1), 49-55.

Lee, S.-J., & Choi, Y.-S. (2008): Decrement of spanwise vortices by a drag-reducing riblet surface. *Journal of Turbulence,* 9(23), 1–15.

Lian, D., & Meelan, C. (2012): Effects of Riblets on Skin Friction and Heat Transfer in High-Speed Turbulent Boundary Layers *50th AIAA Aerospace Sciences Meeting including the New Horizons Forum and Aerospace Exposition*: American Institute of Aeronautics and Astronautics.

Lian, D., & Meelan, C. (2014): Direct Numerical Simulations of High-Speed Turbulent Boundary Layers over Riblets *52nd Aerospace Sciences Meeting*: American Institute of Aeronautics and Astronautics.

Liu, K., & Jiang, L. (2012): Bio-Inspired Self-Cleaning Surfaces. *Annual Review of Materials Research,* 42(1), 231-263.

Moalem-Maron, D., Semiat, R., & Sideman, S. (1980): Enhanced heat transfer in horizontal evaporator- condensers with straight-edged grooved tubes. *Desalination,* 34(3), 289-309.

Naterer, G. F., Glockner, P. S., Thiele, D., Chomokovski, S., Venn, G., & Richardson, G. (2005): Surface micro-grooves for near-wall exergy and flow control: application to aircraft intake de-icing. *Journal of Micromechanics and Microengineering,* 15(3), 501.

Nishimoto, S., & Bhushan, B. (2012): Bioinspired self-cleaning surfaces with superhydrophobicity, superoleophobicity, and superhydrophilicity. *RSC Advances,* 3(3), 671-690.

Park, S.-R., & Wallace, J. M. (1994): Flow alteration and drag reduction by riblets in a turbulent boundary layer. *AIAA Journal,* 32(1), 31-38.

Prince, J. F., Maynes, D., & Crockett, J. (2014): Pressure Drop Measurements for Turbulent Channel Flow over Superhydrophobic Surfaces with Superimposed Riblets. *Paper presented at the ASME 2014 12th International Conference on Nanochannels, Microchannels and Minichannels*,Chicago, Illinois, USA

Reidy, L., & Anderson, G. (1988): Drag reduction for external and internal boundary layers using riblets and polymers *26th Aerospace Sciences Meeting*: American Institute of Aeronautics and Astronautics.

Snarski, S. R., & Lueptow, R. M. (1995): Wall pressure and coherent structures in a turbulent boundary layer on a cylinder in axial flow. *J. Fluid Mech.*, 286, 137-171.

Thomas, A. S. W., & Bull, M. K. (1983): On the role of wall-pressure fluctuations in deterministic motions in the turbulent boundary layer. *J. Fluid Mech.*, 128, 283-322.

Walsh, M. J. (1982): Turbulent boundary layer drag reduction using riblets *20th Aerospace Sciences Meeting*. USA: American Institute of Aeronautics and Astronautics.

Wang, J., Lan, S., & Chen, G. (2000): Experimental study on the turbulent boundary layer flow over riblets surface. *Fluid Dynamics Research*, 27(4), 217-229.

Wang, K., Song, B., & Pan, G. (2005): Drag Reduction of Riblets-Surface of Underwater Vehicle. *Mechanics and Engineering*, 27(2).

Wilkinson, S. P., & Lazos, B. S. (1988): Direct Drag and Hot-Wire Measurements on Thin-Element Riblet Arrays. In H. W. Liepmann & R. Narasimha (Eds.), *Turbulence Management and Relaminarisation* (pp. 121-131). Bangalore, India: Springer Berlin Heidelberg.

Worgull, M. (2009): Chapter 9 - Microstructured Mold Inserts for Hot Embossing *Hot Embossing* (pp. 283-306). Boston: William Andrew Publishing.

Xu, X., & Carey, V. P. (1990): Film evaporation from a micro-grooved surface - An approximate heat transfer model and its comparison with experimental data. *J. Thermophys Heat Transfer*, 4(4), 512-520.

Yulia, P., Pierre, S., & Yves, C. (2008): Turbulent Drag Reduction Using Sinusoidal Riblets With Triangular Cross-Section. *Paper presented at the 38th Fluid Dynamics Conference and Exhibit*,Seattle, Washington.